Available online at www.sciencedirect.com

ScienceDirect

Ceramics International 39 (2013) 8767–8771

CERAMICS INTERNATIONAL

www.elsevier.com/locate/ceramint

Low temperature synthesis of nano-crystalline gadolinium titanate by molten salt route

N. Dharuman[a], L. John Berchmans[b,*]

[a]Department of Chemistry, Urumu Dhanalakshmi College, Tiruchirappalli 620019, India
[b]Electropyrometallurgy Division,Central Electro Chemical Research Institute, Karaikudi 630006, India

Received 9 July 2012; received in revised form 16 April 2013; accepted 17 April 2013
Available online 30 April 2013

Abstract

Nano-crystalline Gadolinium Titanate ($Gd_2Ti_2O_7$) powder was successfully synthesized by "**Single Step Molten Salt Technique**". LiCl–KCl eutectic mixture was used as a molten medium for the reaction. The duration of the synthesis was 10 h. Stoichiometric proportion of the reactants were mixed in an (LiCl–KCl) eutectic medium and treated at 750 °C in an electrical resistance furnace. Single phase Gadolinium Titanate compound was obtained by the thermal process. The synthesized powders were characterized using XRD, FT-IR, UV, EDAX and XPS analyses. The morphology of the powder was examined using SEM and TEM techniques. From the above studies, it has been concluded that pure crystalline Gadolinium Titanate powders can be synthesized via low temperature molten salt process.

Keywords: B. Electron microscopy; E. Nuclear applications; Molten salt method

1. Introduction

Pyrochlore compounds are considered as potential multifunctional materials, which find various technological applications in the areas such as piezoelectricity, ferro and ferrimagnetism, luminescence, giant magneto-resistance and nuclear waste immobilization. Properties of pyrochlore oxides widely vary from insulators or semiconductors to compounds with high ionic, electronic or mixed conductivity making them possible for monolithic fuel cells and gas sensors [1–3].

Compounds exhibiting the pyrochlore structure have been extensively investigated, especially for their properties of anion and mixed conduction [4,5], magneto-resistance and superconductivity. Many applications of these materials have been envisaged as sensors and transistors [6], dielectrics and fast ion conductors [4,7], electrocatalysts [8] and nuclear waste encapsulation [9]. In particular, titanate and stannate pyrochlores have been synthesized for over 40 years [10], and hence a profound knowledge of their structural trends [11], thermodynamic properties [12], disorders [13,14] and non-stoichiometry [15] exist in the literature.

Titanate pyrochlore, $A_2Ti_2O_7$, materials are important, because of their potential use as solid electrolytes and mixed ionic/electronic conducting electrodes [16–20], catalysts and ferroelectric/dielectric device components [21].

Rare-earth pyrochlore ($Gd_2Ti_2O_7$) has been synthesized by different methods such as sol–gel [22–24], solid state reaction [25,26], chemical-coprecipitation, calcinations method [27], single crystal growth [28–30], conventional mixed metal oxide method [31] and Pechini process. However, these methods (except in the case of single crystal growth method) involve multi-step complicated reaction routes with longer duration for synthesis. These reactions result in non-homogenous polycrystals with irregular morphology and broad particle size distribution. Furthermore, higher calcination temperature is needed to obtain a single phase compound. Single crystal growth method involves sophisticated instrumentation. To overcome all these disadvantages, we have made an attempt through a novel molten salt method (MSM) to synthesize high purity Gadolinium Titanate ($Gd_2Ti_2O_7$) compound.

In this method, the molten salt is used as the reaction medium, where the reactants are dissolved, producing pure compounds of interest. Since, the rate of diffusion of reactants

*Corresponding author. Tel.: +91 4565 227550 9 (O), +91 4565 229374 (R), Mobile: +91 9487035110; fax: +91 4565 227779.
E-mail addresses: ljberchmans@gmail.com, berchmans@cecri.res.in (L. John Berchmans).

0272-8842/$ - see front matter © 2013 Elsevier Ltd and Techna Group S.r.l. All rights reserved.
http://dx.doi.org/10.1016/j.ceramint.2013.04.063

in the molten melt is much higher than those in the solid-state reaction, the homogeneous oxide materials are formed at an accelerated rate. In this study, we report the preparation of nano-crystalline $Gd_2Ti_2O_7$ compound using Gadolinium oxide (Gd_2O_3) and Metatitanic acid (H_2TiO_3) as the reactants. LiCl–KCl eutectic salt mixture was used as a flux during the synthesis process.

2. Experimental procedure

2.1. Synthesis of $Gd_2Ti_2O_7$ powders

Gadolinium oxide (98% purity, Aldrich), and Metatitanic acid (Travancore Titanium Products Limited, Kerala, India) were used as the starting materials for the synthesis. The reactants were mixed in stoichiometric proportions and thoroughly ground using mortar and pestle. An equimolar mixture of lithium chloride and potassium chloride salts were used as the flux. The reactants and the flux were placed in an high density alumina crucible and fired at 750 °C for 10 h. At this temperature, the salt medium forms a molten flux, and the precursor oxides disperse, dissociate, rearrange, and diffuse rapidly throughout the melt forming the final product. Finally, the resultant product was washed with dilute hydrochloric acid (10%) followed by hot distilled water for several times. Then the residue was dried at 50 °C for 15 min to remove the surface moisture, yielding a free flowing fine crystalline white powder.

$$Gd_2O_3 + 2H_2TiO_3 \rightarrow Gd_2Ti_2O_7 + 2H_2O$$

2.2. Characterization

XRD analysis was carried out using an X-ray powder diffractometer (Philips 8030 X-ray Diffractor) with Cu Kα radiation ($\lambda = 1.5406$ Å). The XRD patterns were compared with the standard JCPDS: (23-0259) files. FTIR measurements were performed with a Perklin Elmer UK paragon-500 spectroscope in the mid infrared region (4000–400 cm^{-1}). For each sample preparation, approximately 2 mg of sample was dispersed in 300 mg of KBr powder and pressed into a pellet and used for the analysis. The elemental analysis of the powders was done using the energy dispersive X-ray analysis (EDAX) technique. This analytical tool was an attachment to the SEM (scanning electron microscope) unit. The surface morphology was analyzed by using a scanning electron microscopy (JEOL-JSM-3.5 CF-JAPAN).The nano-size of the powder was assessed by a transmission electron microscope. TEM images were recorded using a JEOL-3010 transmission electron microscope using 300 kV accelerating voltage with a 400-mesh ultrathin carbon type A copper grid.

3. Results and discussion

3.1. X-ray diffraction

Fig. 1 shows the X-ray diffraction patterns of synthesized $Gd_2Ti_2O_7$ powders obtained by the molten salt route. The diffraction peaks of the samples can be indexed as spinel Gadolinium Titanate. From the XRD data, the lattice constant 'a' was calculated using the formula

$$a = d\sqrt{h^2 + k^2 + l^2}$$

where d is the inter-planar spacing (Å) and h, k, l are the Miller indices. XRD patterns of the synthesized polycrystalline powders show characteristic reflections of $Gd_2Ti_2O_7$ pyrochlore type crystal strcture. The main reflections observed correspond to (222), (440) and (622) planes with the $2\theta \sim 30^\circ$ (100% relative intensity), and weak peaks at 50.12° (50%) and 60.198 (60%) are confirming the presence of $Gd_2Ti_2O_7$ pyrochlore compound. Few peaks appearing in the spectrum can be assigned to the presence of rutile TiO_2. The presence of rutile TiO_2 phase does not have any influence on the pyrochlore phase [26].

The unit cell parameters have been determined from the XRD data and found to be 10.1687 Å. This calculated lattice constant value is in good agreement with the standard JCPDS data ($a = 10.1860$ Å) [4]. The line broadening of the diffraction peaks has been ascribed to the fact that the synthesized powders have nano-structured morphology. The average crystalline size of the powder was determined by using Debye–Scherrer's formula

$$D = 0.9\lambda/(\beta cos\ \theta)$$

where $\beta = \Delta/2$ (Δ is the full width at half maximum for a given diffraction peak), λ = wavelength of the Cu Kα radiation and (wave length $\lambda_{Cu} = 1.5406$ Å), and θ = Bragg's angle.

The average crystalline size of the particles is found to be in the range of 31–39 nm.

3.2. FT-IR spectroscopy

The FT-IR spectrum of the single phase $Gd_2Ti_2O_7$ compound is shown in Fig. 2. FT-IR bands have been analyzed for identifying the functional groups present in the compound. From the FT-IR spectrum, it is perceived that the absorption bands appearing between 1700 and 2400 cm^{-1} correspond to

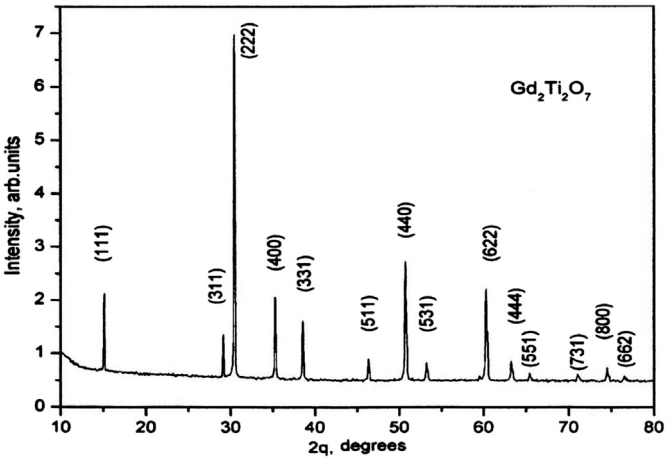

Fig. 1. X-ray diffraction pattern of $Gd_2Ti_2O_7$ Powder.

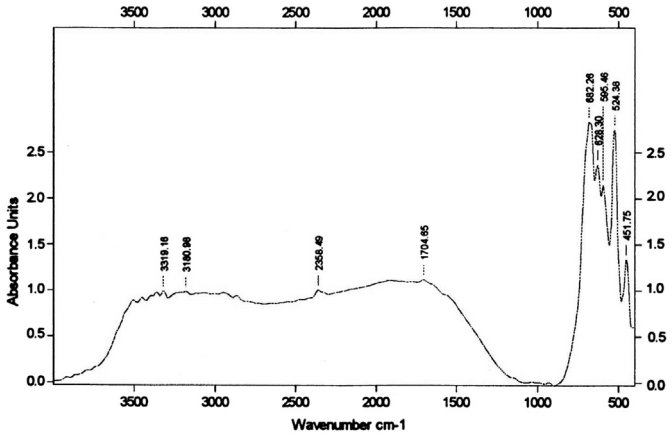

Fig. 2. FT-IR spectrum of $Gd_2Ti_2O_7$ powders.

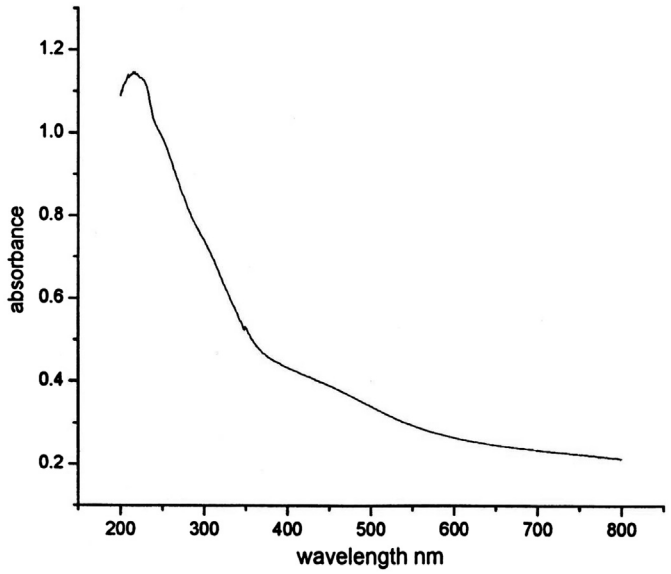

Fig. 3. UV–vis absorption spectrum of $Gd_2Ti_2O_7$.

the Ti–O stretching vibration mode. The bands appearing between 500 and 900 cm^{-1} can be attributed to Ti–O–Ti bending vibrations. At higher wave length region namely 3200–3500 cm^{-1}, the spectrum reveals the presence of hydroxyl group in the synthesized compound.

From the spectral data, we may unambiguously assign the bands near 519–526, 330 and 306–312 cm^{-1} to A_{1g}, E_g and F_{2g} modes. This data are consistent with the experimental and theoretical studies made by Saha et al.[32]. From the crystal-ochemical point of view, they might be regarded as vacancy-ordered defect fluorites with geometrical frustration in $RE_2Ti_2O_7$ pyrochlores (RE=rare earth). It may arise from the distribution of the RE^{3+} magnetic ions, positioned at the vertices of a corner-linked tetrahedral network [26].

3.3. UV–vis spectroscopy analysis

The UV–vis spectroscopy analysis is used to calculate the band gap energy of the material with the help of the absorption edge wavelength and cut-off wavelength of the absorption spectrum. The recorded UV spectrum is shown in Fig. 3. From the absorbance spectrum, we can calculate the energy band gap as follows.

4. Calculation of energy band gap (eV)

The band gap energy was calculated using the data obtained from the optical measurements by using the following equation [33]:

$$(\alpha h\nu)^2 = A(h\nu - E_g)$$

where α—absorption coefficient, A—optical constant, and E_g—band gap energy.

Band gap energy (E_g) was calculated from the UV–vis spectrum by extrapolating a straight line from the absorption curve to the abscissa. When $\alpha=0$, then $E_g=h\nu$.

The band gap energy of Gadolinium Titanate is determined from the graph and found to be 5.7 eV.

The main absorption bands are located within the region of 200–400 nm, which are assigned to the absorption in the titanate group framework. The different phase compositions and the crystal structure have no influence on the main absorption band, suggesting that the TiO_6 produces the energy absorption for these compounds [23].

4.1. XPS analysis of $Gd_2Ti_2O_7$

The X-ray photoelectron spectroscopy is used for the characteristic changes in the chemical environment of an element in a structure, especially in the case of amorphous materials.The recorded XPS spectrum is presented in Fig. 4.The binding energy vs the intensity of O 1*s* spectrum has shown two obvious peaks. This inference is consistent with the two types of O^{2-} coordination geometries in the $Gd_2Ti_2O_7$ pyrochlore.

When the pyrochlore oxides are subjected to ion irradiation, the cation disordering between the A and B sites occurs, thus the chemical environment of all of the oxygen anions becomes more similar. XPS results support the link between cation and anion disordering.

According to the pyrochlore structure, there are two types of cation–anion bonds, namely Ti–O, and Gd–O. Considering the lower electronegativity of Gd^{3+} as compared with that of Ti^{4+}, the ionic character of the Gd–O bond is greater than that of the Ti– bond. Thus, the peak of O 1*s* spectrum with low binding energy to oxygen anions bonded to gadolinium, while the peak of O 1*s* spectrum with the higher binding energy is assigned to Ti–O.

In the XPS spectrum, the components of $Ti–O_2$ are observed at 460.20 and 465.20 eV respectively because of the spin orbital splitting. This observation confirms the presence of gadolinium is in 3+ states in the synthesized $Gd_2Ti_2O_7$ compound. The XPS data are in good agreement with the reported literature data [34].

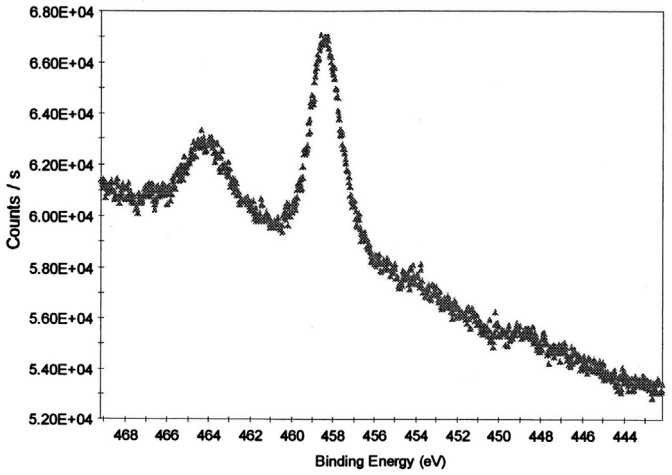

Fig. 4. XPS spectrum of $Gd_2Ti_2O_7$.

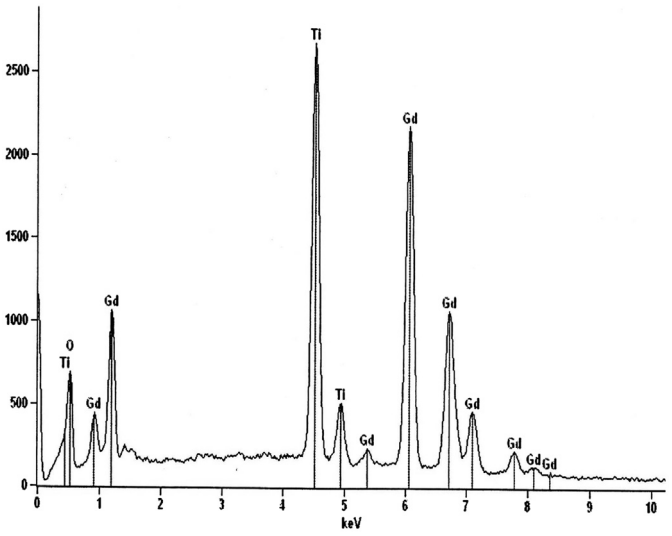

Fig. 5. EDAX analysis of $Gd_2Ti_2O_7$ powders.

4.2. EDAX analysis

The elemental analysis of the synthesized powders was performed using the energy dispersive X-ray analysis (EDAX) technique. The EDAX spectrum is presented in Fig. 5. The EDAX spectrum indicates, the constituent elements are in appropriate proportions in the synthesized compound. This information reveals that the prepared compound is in pure form without much impurity phases. The quantitative analysis of synthesized nano-crystalline gadolinium titanate is presented in the Table 1.

4.3. SEM analysis

The morphological features of the powders were obtained by means of scanning electron microscopy. Fig. 6(a,b) shows the SEM-micrographs of the synthesized $Gd_2Ti_2O_7$ powders obtained by molten salt technique.

The SEM images reveal the cubic crystal morphology at higher magnification. Molten salt synthesis produces enhanced crystal morphology devoid of agglomeration of particles. The square column-like morphology with good crystal state can be found, whose particle size can be determined to be around 5–10 μm.

4.4. Transmission electron microscopy (TEM)

Transmission Electron Micrographs (TEM) have been recorded to show that the synthesized powders are nano-crystalline in nature. The TEM micrographs are shown in Fig. 7(a,b) suggesting that the crystalline size is in the range of 200 nm.

TEM analysis shows near-cubic crystalline particles with an average size of 200 nm. The faces of these nano-crystals are mostly in globular form. In other words, the formation of

Table 1
Quantitative results: $Gd_2Ti_2O_7$.

Element	Net count	Weight (%)	Atom (%)
O	4547	2.29	47.25
Ti	39,342	20.63	26.50
Gd	58,520	67.08	26.25
Total		100.0	100.00

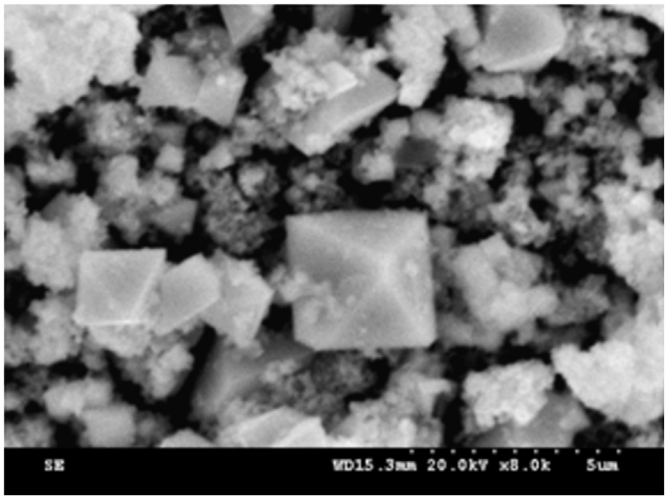

Fig. 6. (a,b) SEM images of the synthesized $Gd_2Ti_2O_7$ powders.

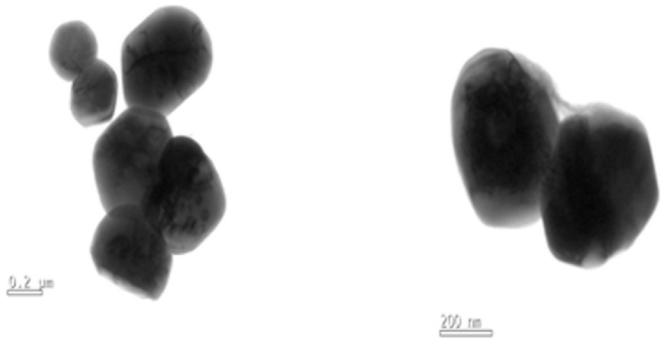

Fig. 7. (a,b) TEM images of $Gd_2Ti_2O_7$ powders.

$Gd_2Ti_2O_7$ nanocrystals is likely a kinetic and morphological manifestation of the initial nuclei of the cubic form [35].

5. Conclusions

Nano-structured Gadolinium Titanate powders are successfully synthesized by single step low temperature molten salt route. Thus the molten salt synthesis (MSS) has been found to be a versatile technique for the synthesis of pure crystalline, $Gd_2Ti_2O_7$ powders which can be used for the nuclear waste encapsulation applications.

Acknowledgments

The authors express their sincere gratitude to the Faculty of chemistry and the Management of Urumu Dhanalakshmi College, Tiruchirappalli, Tamilnadu for their encouragement to carry out this work. The authors also sincerely thank The Director, CECRI, Staff of EPM Division and Scientists of Characterization Laboratory for their kind help.

References

[1] C. Rodney, J.Ewing William, Weber Jie Lian, Nuclear waste disposal-pyrochlore ($A_2B_2O_7$) Nuclear waste form for the immobilization of plutonium and minor actinides, Journal of Applied Physics 95 (2004) 5949–5971.
[2] S.A. Kramer, H.L. Tuller, A novel titanate-based oxygen ion conductor $Gd_2Ti_2O_7$, Solid State Ionics 82 (1995) 15–23.
[3] C. Heremans, B.J. Wuensch, J.K. Stalick, E. Prince, Fast-ion conducting $Y_2(Zr_yTi_{1-y})_2O_7$ pyrochlores neutron rietveld analysis of disorder induced by Zr substitution, Journal of Solid State Chemistry 117 (1995) 108–121.
[4] M.A. Subramanian, G. Aravamudan, G.V. Subba Rao, Oxide pyrochlore, Progress in Solid State Chemistry 15 (1983) 55–143.
[5] O. Porat, C. Heremans, H.L. Tuller, Stability and mixed ionic electronic conduction in $Gd_2(Ti_{1-x}Mo_x)_2O_7$ under anodic conditions, Solid State Ionics 94 (1997) 75–83.
[6] J.B. Goodenough, R.N. Castellano, Defect pyrochlores as catalyst supports, Journal of Solid State Chemistry 44 (1982) 108–112.
[7] P.P. Rao, S.J. Liji, K.R. Nair, P. Koshy, New pyrochlore-type oxides in Ca–R–Ti–Nb–O system (R = Y, Sm or Gd)-structure, FT-IR spectra and dielectric properties, Materials Letters 54 (2004) 1924–1927.
[8] Ismunandar, B.J. Kennedy, B.A. Hunter, Bonding and structural variations in doped $Bi_2Sn_2O_7$, Journal of Solid State Chemistry 131 (1997) 317–325.
[9] E.J. Harvey, K.R. Whittle, G.R. Lumpkin, R.I. Smith, S.A.T. Redfern, Solid solubilities of (La Nd,)$_2$(Zr,Ti)$_2O_7$ phases deduced by neutron diffraction, Journal of Solid State Chemistry 178 (2005) 800–810.
[10] L.H. Brixner, Structural and luminescent properties of the $Ln_2Hf_2O_7$-type rare earth hafnates, Materials Research Bulletin 19 (1984) 143–149.
[11] B.J. Kennedy, B.A. Hunter, C.J. Howard, Structural and bonding trends in tin pyrochlore oxides, Journal of Solid State Chemistry 130 (1997) 58–65.
[12] K.B. Helean, S.V. Ushakov, C.E. Brown, A. Navrotsky, J. Lian, R.C. Ewing, Formation enthalpies of rare earth titanate pyrochlores, Journal of Solid State Chemistry 177 (2004) 1858–1866.
[13] L. Minervini, R.W. Grimes, Lanthanum pyrochlores and the effect of yttrium addition in the systems, Journal of the American Ceramic Society 83 (2000) 1873–1878.
[14] C. Heremans, B.J. Wuensch, J.K. Staick, E. Prince, Fast-ion conducting $Y_2(Zr_yTi_{1-y})_2O_7$ pyrochlores neutron Rietveld analysis of disorder induced by Zr substitution, Journal of Solid State Chemistry 117 (1995) 108–121.
[15] C.R. Stanek, L. Minervini, R.W. Grimes, Nonstoichiometry in $A_2B_2O_7$ pyrochlores, Journal of the American Ceramic Society 85 (2002) 2792–2798.
[16] S. Kramer, M. Spears, H.L. Tuller, Formation enthalpies of rare earth titanate pyrochlores, Solid Oxide Fuel Cells Symposium Proceedings 119 (1993) 93–94.
[17] S.A. Kramer, H.L. Tuller, A novel titanate-based oxygen ion conductor Gd_2Ti_2O, Solid State Ionics 82 (1995) 15–23.
[18] P.K. Moon, H.L. Tuller, Ionic conduction in the $Gd_2Ti_2O_7$–$Gd_2Zr_2O_7$ system, Solid State Ionics 28–30 (1988) 470–474.
[19] P.J. Wilde, C.R.A. Catlow, Defects and diffusion in pyrochlore structured oxides, Solid State Ionics 112 (1998) 173–183.
[20] P.J. Wilde, C.R.A. Catlow, Molecular dynamics study of the effect of doping and disorder on diffusion in gadolinium zirconate, Solid State Ionics 112 (1998) 185–195.
[21] J.H. Lee, Y.M. Chiang, Pressure-induced pyrochlore-perovskite phase transformation in PLZST ceramics, Journal of Electroceramics 6 (1) (2001) 7–12.
[22] Ying Zhang, Linghong Ding, Xinling Pang, Weifeng Zhang, Influence of annealing temperature on luminescent properties of Eu^{3+}/V^{5+} co-doped nanocrystalline $Gd_2Ti_2O_7$ powders, Journal of Rare Earths 27 (2009) 900–904.
[23] Lin Lixia, Yan Bing, Rare earth titanates ceramics $Na_2La_2Ti_3O_{10}$:Pr^{3+} and $Re_2Ti_2O_7$:Pr^{3+} (R = Gd, Y): sol–gel synthesis, characterization and luminescence, Journal of Materials Science Materials in Electronics 22 (2011) 672–678.
[24] M.L. Pang, J. Fu, Z.Y. Cheng, Luminescent properties of $Gd_2Ti_2O_7$:Eu^{3+} phosphor films prepared by sol–gel process, Materials Research Bulletin 39 (2004) 1607–1614.
[25] Dan S. Perera, Martin W.A. Stewart, Huijun Li, R. Arthur Day, Eric R. Vance, Tentative phase relationships in the system $CaHfTi_2O_7$–$Gd_2Ti_2O_7$ with up to 15 mol% additions of Al_2TiO_5 and $MgTi_2O_5$, Journal of the American Ceramic Society 85 (12) (2002) 2919 -243.
[26] M. Maczka, J. Hanuza, K. Hermanowicz, A.F. Fuentes, K. Matsuhira, Z. Hiroi, Temperature-dependent Raman scattering studies of the geometrically frustrated pyrochlores $Dy_2Ti_2O_7$, $Gd_2Ti_2O_7$ and $Er_2Ti_2O_7$, Journal of Raman Spectroscopy 39 (2008) 537–544.
[27] Z.G. Liu, J.H. Ouyang, K.N. Sun, Electrical conductivity improvement of $Nd_2Ce_2O_7$ ceramic co-doped with Gd_2O_3 and Zro_2, Fuel Cells 11 (2) (2011) 153–157.
[28] S.S. Sosin, A.I. Smirnov, L.A. Prozorova, G. Balakrishnan, M.E. Zhitomirsky, Novel magnetic phases in a $Gd_2Ti_2O_7$ pyrochlore for a field applied, Physical Review B 73 (2006) 212402–212407.
[29] S.S. Sosin, L.A. Prozorova, A.I. Smirnov, P. Bonville, G. Jasmin-Le Bras, O.A. Petrenko, Spin dynamics of the pyrochlore magnets $Gd_2Ti_2O_7$ and $Gd_2Sn_2O_7$ in the paramagnetic state, Physical Review B 77 (2008) 104424–104432.
[30] E. Morosan, J.A. Fleitman, Q. Huang, J.W. Lynn, Y. Chen, X. Ke, M.L. Dahlberg, P. Schiffer, C.R. Craley, R.J. Cava, Structure and magnetic properties of the $Ho_2Ge_2O_7$ pyrogermanate, Physical Review B **77** (2008) 224423–224430.
[31] F. Matteucci, G. Cruciani, M. Dondi, G. Baldi, A. Barzanti, Crystal structural and optical properties of Cr-doped $Y_2Ti_2O_7$ and $Y_2Sn_2O_7$ pyrochlores, Acta Materialia 55 (2007) 2229–2238.
[32] S. Saha, D.V.S. Muthu, C. Pascanut, N. Dragoe, R. Suryanarayanan, G. Dhalenne, A. Revcolevschi, S. Kurmakar, S.M. Sharma, A.K. Sood, High-pressure Raman and X-ray study of the spin-frustrated pyrochlore $Gd_2Ti_2O_7$, Physical Review B 74 (2006) 64109–64117.
[33] M.-M. Bagheri-Mohagheghi, N. Shahtahmasebi, M.R. Alinejad, A. Youssefi, M. Shokooh-Saremi, The effect of the post-annealing temperature on the nano-structure and energy band gap of SnO_2 semiconducting oxide nano-particles synthesized by polymerizing–complexing sol–gel method, Physica B 403 (2008) 2431–2437.
[34] J. Chen, J. Lien, L.M. Wang, R.C. Ewing, X-ray photoelectron spectroscophy study of irradiation-induced amorphization of $Gd_2Ti_2O_7$, Applied Physics Lettters 79 (13) (2001) 1989–1991.
[35] Mao Yuanbing, Guo Xia, Jian Y. Huang, Kang L. Wang, Jane P. Chang, Luminescent nanocrystals with $A_2B_2O_7$ composition Synthesized by a kinetically modified molten salt method, Journal of Physical Chemistry 113 (2009) 1204–1208.